Список літератури: 1. *Реклейтис Г., Рейвиндран А., Рэгсдел К.* Оптимизация в технике. Т. 1. – М.: Мир, 1986. **2.** *Михлик С.Г.* Линейные уравнения в частных производных. – М.: Высшая школа, 1977. **3.** *Грищенко В. М., Галаган Ю.М.* Алгоритм чисельної оптимізації конструкцій з урахуванням обмежень за допомогою R-функцій // Вісник НТУ «ХПІ». Тематичний випуск: Динаміка та міцність машин. – Харків: НТУ «ХПІ», 2006. – № 32. – С. 67-77.

Надійшла до редколегії 21.08.2009

УДК 539.3

S.GLADKOV, TU Dortmund;
M.STIEMER, Dr.rer.nat, TU Dortmund;
A.GROSSE-WOEHRMANN, TU Dortmund;
B.SVENDSEN, Dr.rer.nat., TU Dortmund

NUMERICAL MODELING OF PHASE-SEPARATION IN BINARY MEDIA BASED ON THE CAHN-HILLIARD EQUATION

У статті описано процедуру наближеного рішення рівняння Кана-Хіллярда в частинних похідних 4го порядку котра базується на явному методі Ейлера в часі та змішаній постановці з білінійними скінченими елементами в просторі. Наведено чисельні рішення для ідеалізованої моделі з двуямним потенціалом (в 2-х та 3-х просторових вимірах) та більш фізично релевантної моделі з логарифмічним потенціалом (тільки в 2-х просторових вимірах).

In the article numerical procedure for solution of the Cahn-Hilliard equation which is based on the forward Euler method in time and mixed (due to 4th order nature of differential operator) linear finite element formulation in space is described. Numerical examples consist of idealized model with double well potential (in 2 and 3 spatial dimensions) and more physically relevant model with logarithmic potential (in 2D only).

1. Introduction and motivation. During industrial hot forming processes such as extrusion, hot rolling or hot forging materials undergo mechanical deformation and recrystallization. For particular case of extrusion (Fig. 1) one can observe precipitate formation during the last, cooling stage of the extrusion process. Usually above mentioned phenomena influence each other in a complicated way, and it is exactly this influence of recrystallization/precipitate formation on a material's ductility and strength that effects the appeal of a hot forming method.

Precipitates form a separate phase in the alloy. A reliable simulation based prediction of forming results hence requires a coupled model for the evolution of both the mechanical fields and the evolution of areas covered by different phases.

While first attempts on the finite element simulation of phase-field models have recently been presented in [1, 2, 3, 4], their consideration in the context of a structural mechanical finite element simulation is a new issue [5, 6, 7, 8, 9, 10].

The purpose of this work is the formulation and application of a continuum field approach to the phenomenological modeling of the behavior of technological alloys undergoing phase transitions and attendant inelastic deformation. In the current paper only first results on the numerical modeling of the phase separation in the idealized binary media solely are presented. This is the continuation of the work started in [11].

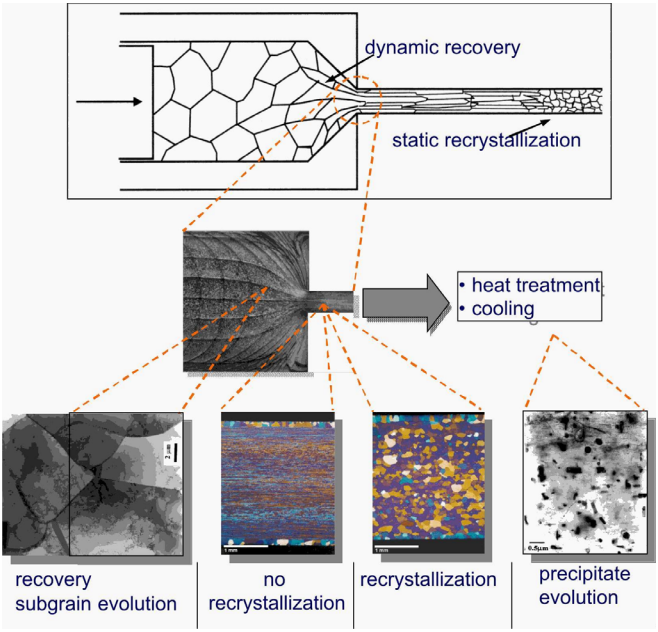

Figure 1 – Schematic extrusion process

2. Model formulation. To describe the phase transition, so called phase-field approach is utilized [12, 13, 14]. It can be motivated as follows. The interface between two phases on the atomic scale is a «mushy» one (Fig. 2). The classical approach to model this interface on the meso scale is to use a sharp interface model although this kind of the problem statement might be numerically quite complicated because one must impose boundary conditions on the moving interface (so-called Stefan conditions). Contrary to this approach, we will use a relaxed (or diffused) interface model proposed in [15] where different phases are distinguished using a phase-field – a field defined on the whole domain of the simulation and serving as a relaxed characteristic function for each phase. In this particular case of Cahn-Hilliard model the same quantity – concentration – serves both as a physical concentration and as phase indicator.

In this paper Cahn-Hilliard equation with two types of free energies is consid-

ered: with idealized double-well potential and with more physically relevant logarithmic potential. Because this equation is 4th order partial differential equation, but we want to stay with numerically efficient linear finite elements, mixed formulation is employed.

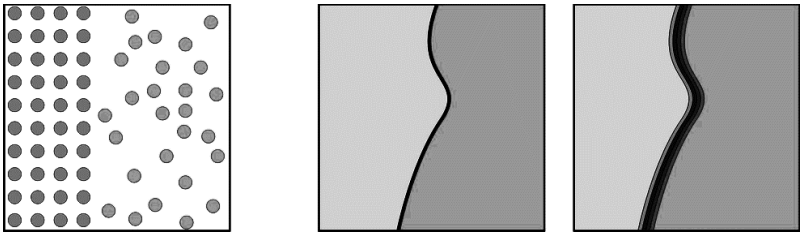

Figure 2 – «Mushy» interface on the atomic scale (*left*) and sharp and relaxed interfaces on the meso scale (*right*)

2.1 Cahn-Hilliard equation polynomial free energy (double well potential). This simplified nondimensionalized Cahn-Hilliard equation is taken from [16]:

$$\dot{c} = D\Delta\left(c^3 - c - \gamma\Delta c\right), \tag{1}$$

where $-1 \le c \le 1$ is concentration, D is a diffusion coefficient and γ is square of length of the transition region between the phases. Here $F_c = \frac{1}{4}c^4 - \frac{1}{2}c^2 + a$ can be identified as chemical free energy (Fig. 3), $F_\gamma = \frac{\gamma}{2}\nabla c \cdot \nabla c$ as surface free energy, $\mu = \mathrm{D}_c(F_c + F_\gamma) = c^3 - c - \gamma\Delta c$ as a chemical potential and $\boldsymbol{j} = D\nabla\mu$ as mass diffusion flux. Here the notation $\mathrm{D}_x(\cdot)$ for derivative of function $(\cdot)$ with respect to its argument x is used. Problem statement should be closed with the homogeneous Neumann boundary conditions:

$$\begin{aligned} \boldsymbol{n}\cdot\boldsymbol{j} &= 0, \\ \boldsymbol{n}\cdot\nabla c &= 0, \end{aligned} \tag{2}$$

and random initial conditions for concentration in the range [–1, 1].

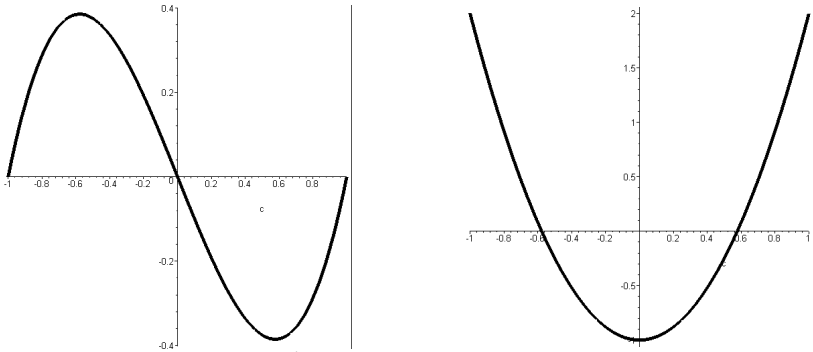

Figure 3 – 1st (*left*) and 2nd (*right*) derivatives of the chemical free energy F_c

Mixed formulation of problem (1) is

$$\begin{aligned} \dot{c} &= D\left[\Delta c^3 - \Delta\psi\right], \\ \psi &= c + \gamma\Delta c, \end{aligned} \tag{3}$$

where now there are 2 unknowns – c and ψ.

For time discretization backward Euler method is used. Time derivative is approximated as $\dot{c} = (c(t) - c(t-\Delta t))/\Delta t$ and new system (not containing time) is:

$$\begin{aligned} c &= c^t + \Delta t D\left[\Delta c^3 - \Delta\psi\right], \\ \psi &= c + \gamma\Delta c, \end{aligned} \tag{4}$$

where c^t is successful solution from the previous time step.

Spatial discretization of equations (4) is performed using Bubnov-Galerkin method. Multiplying equations (4) with test functions $\{c^*,\psi^*\}$, integrating over domain Ω and accounting for boundary conditions (2) we end up with the following weak form in terms of residual:

$$\begin{aligned} r(c,\psi) = \int_\Omega &(c^*c - \Delta t D c^*\Delta c^3 + \Delta t D c^*\Delta\psi - \\ &c^*c^t + \psi^*\psi - \psi^*c - \gamma\psi^*\Delta c)\, d\Omega. \end{aligned} \tag{5}$$

Or using the chain rule $\Delta c^3 = 3c^2\Delta c + 6c\nabla c\cdot\nabla c$ and integration-by-parts:

$$\begin{aligned} r(c,\psi) = \int_\Omega &(c^*c + 3\Delta t D c^2\nabla c^*\cdot\nabla c - \Delta t D\nabla c^*\cdot\nabla\psi - \\ &c^*c^t + \psi^*\psi - \psi^*c + \gamma\nabla\psi^*\cdot\nabla c)\, d\Omega. \end{aligned} \tag{6}$$

To solve this nonlinear system of equations Newton method is used. Newton updates are calculated as $c_{new} = c + \delta c$, $\psi_{new} = \psi + \delta\psi$.

Final linearized system of equations is

$$\mathrm{D}_c r(c,\psi)[\delta c] + \mathrm{D}_\psi r(c,\psi)[\delta\psi] = -r(c,\psi), \tag{7}$$

where

$$\begin{aligned} \mathrm{D}_c r(c,\psi)[\delta c] = \int_\Omega &(c^*\delta c + 6\Delta t D c\nabla c^*\cdot\nabla c\delta c + 3\Delta t D c^2\nabla c^*\cdot\nabla\delta c - \\ &\psi^*\delta c + \gamma\nabla\psi^*\cdot\nabla\delta c)\, d\Omega, \\ \mathrm{D}_\psi r(c,\psi)[\delta\psi] = \int_\Omega &(\psi^*\delta\psi - \Delta t D\nabla c^*\cdot\nabla\delta\psi)\, d\Omega. \end{aligned} \tag{8}$$

It should be mentioned that the notation used here for linear system (7) can in fact be almost *directly* implemented into the open-source finite element library deal.II [17] which is used in this work for all numerical computations.

2.2 Cahn-Hilliard equation with logarithmic free energy. This equation is almost the same as one described in the previous section, but bulk chemical free energy F_c now contain logarithms and taken according to [7] in the form:

$$F_c = g_1 c + g_2(1-c) + g_3 c\ln c + g_4(1-c)\ln(1-c) + g_5 c(1-c). \tag{9}$$

Then procedure is the same as in section 2.1 except that now c has range $[0,1]$

and second derivative of the chemical free energy is singular for $c = 0$ and $c = 1$ (1st and 2nd derivatives of (9) are plotted on Fig. 4). Mixed formulation of this problem (after time discretization via backward Euler method) is

$$\begin{aligned} c &= c^t + \Delta t D \Delta \mu, \\ \mu &= \mathrm{D}_c F_c - \gamma \Delta c, \end{aligned} \tag{10}$$

where as auxiliary variable value of the chemical potential μ is taken. Multiplying equations (10) with test functions $\{c^*, \psi^*\}$, integrating over domain Ω and accounting for boundary conditions (2) following expression is achieved for residual:

$$\begin{aligned} r(c,\psi) = \int_\Omega & (c^* c - c^* c^t + \Delta t D \nabla c^* \cdot \nabla \mu + \\ & \mu^* \mu - \mu^* F_c c - \gamma \nabla \mu^* \cdot \nabla c)\, d\Omega, \end{aligned} \tag{11}$$

where

$$\mathrm{D}_c F_c = g_1 - g_2 + g_3(1 + \ln c) - g_4(1 - \ln(1 - c)) + g_5(1 - 2c). \tag{12}$$

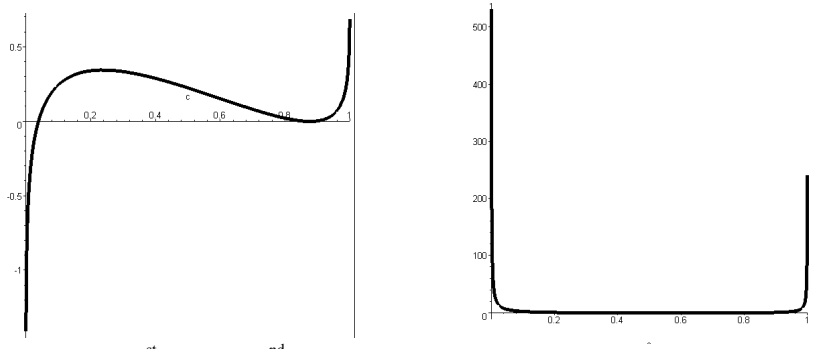

Figure 4 – 1st (*left*) and 2nd (*right*) derivatives of the chemical free energy F_c (9)

To solve nonlinear equation (11) as before Newton method would be used in the form of equation (7) where

$$\begin{aligned} \mathrm{D}_c r(c,\mu)[\delta c] &= \int_\Omega (c^* \delta c - \mu^* \mathrm{D}_c^2 F_c \delta c - \gamma \nabla \mu^* \cdot \nabla \delta c)\, d\Omega, \\ \mathrm{D}_\mu r(c,\mu)[\delta \mu] &= \int_\Omega (\Delta t D \nabla c^* \cdot \nabla \delta \mu + \mu^* \delta \mu)\, d\Omega, \end{aligned} \tag{13}$$

and

$$\mathrm{D}_c^2 F_c = \frac{g_3}{c} + \frac{g_4}{1-c} - 2g_5. \tag{14}$$

3. Numerical results. In this section numerical results are presented for the given in section 2 model.

3.1 Cahn-Hilliard equation polynomial free energy. To perform numerical simulations $D = 1$; $\gamma = 0{,}5$ and $\Omega = [-100; 100]^2$ where chosen. Time step $\Delta t = 0{,}5$, simulation time $t_{final} = 300$ and tolerance for Newton method is set to 10^{-10}. Firstly

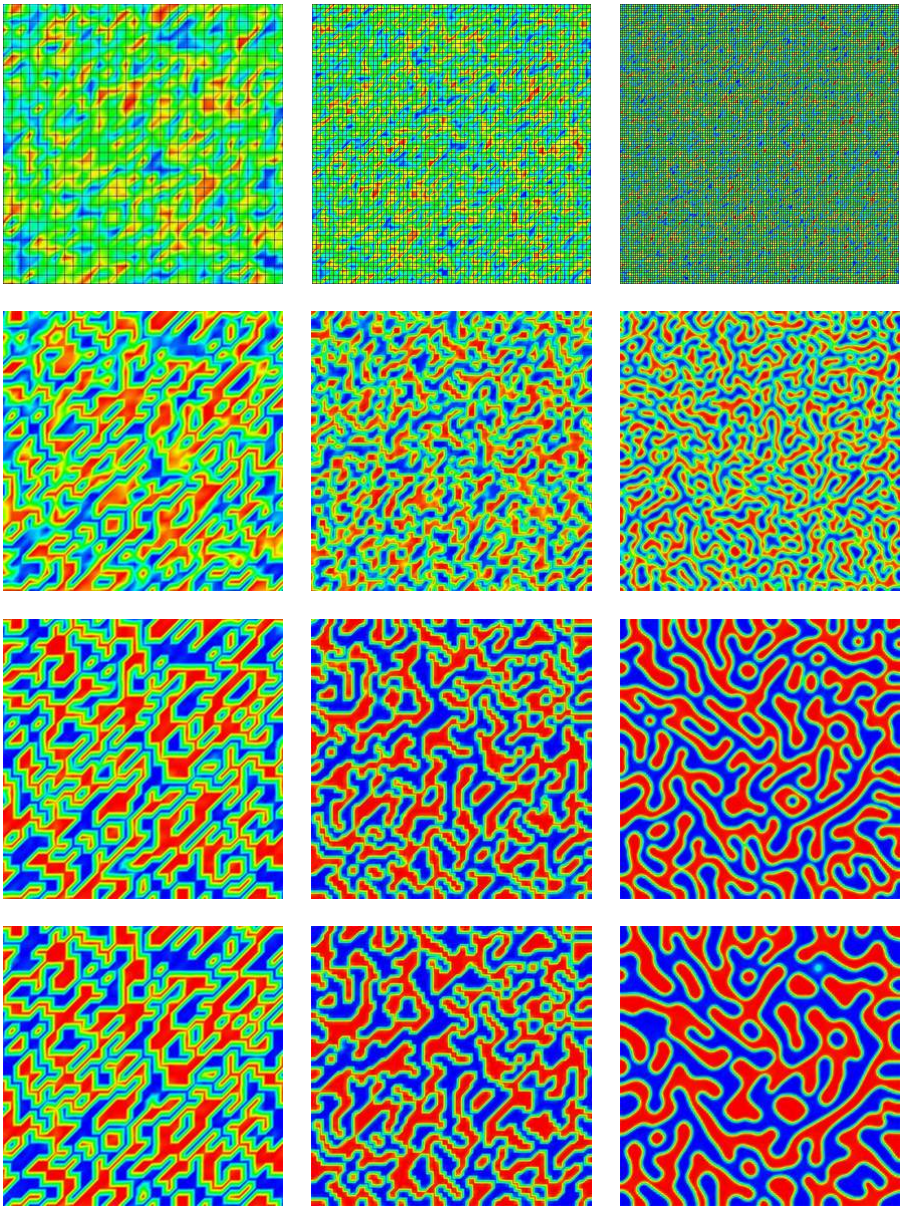

Figure 5 – Solution of the Cahn-Hilliard equation (1,2) using 32^2 (*left*), 64^2 (*middle*) and 128^2 (*right*) elements for time steps (from top to bottom) $t = 50; 150; 300$. Legend: blue $c = -1$, red $c = 1$

solution was tried on various meshes with 32^2, 64^2 and 128^2 finite elements and it is plotted on the Fig. 5. One can see that 32^2 and 64^2 elements is definitely not enough to resolve the problem with the given value of γ correctly.

On Fig. 6 results for different values of parameter $\gamma = 0{,}5;4;16$ are shown on the mesh of 64^2 finite elements. Qualitatively it is observed that the interface becomes thicker and for the value $\gamma = 4$ problem can be resolved with only 64^2 elements.

First attempts to perform simulation in 3D are shown on the Fig. 7 for mesh consisting of 64^3 finite elements where $\Delta t = 0{,}2$; $t_{final} = 200$; $D = 1$ and $\gamma = 1$.

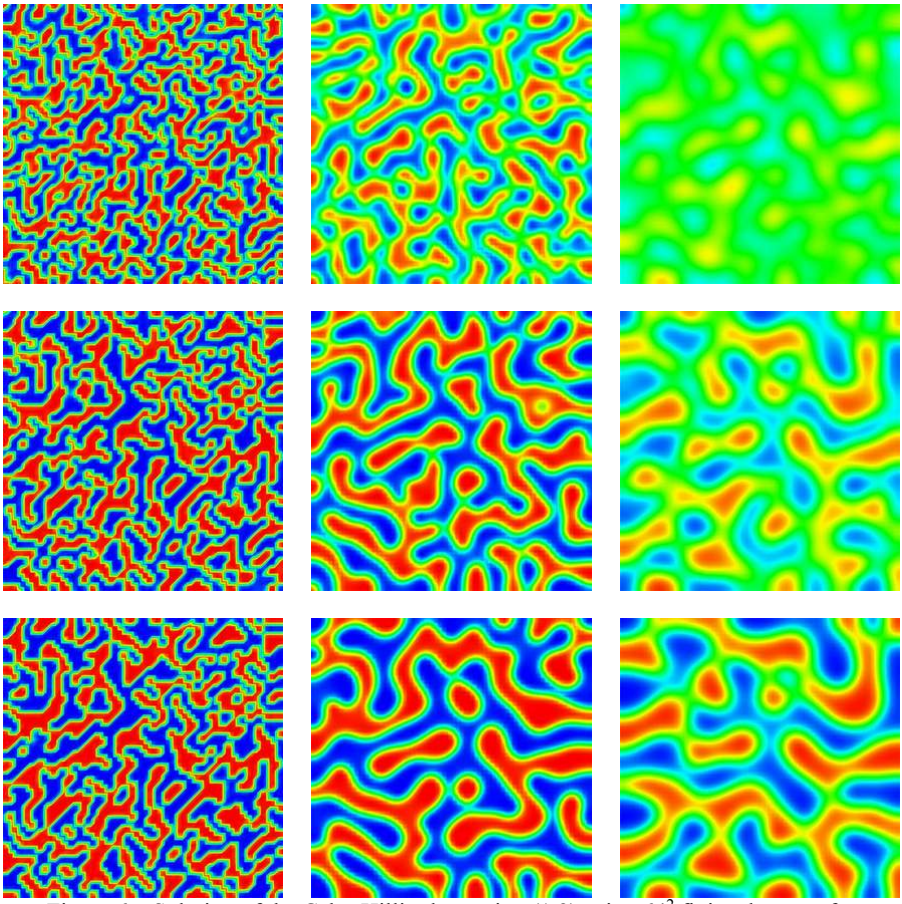

Figure 6 – Solution of the Cahn-Hilliard equation (1,2) using 64^2 finite elements for $\gamma = 0{,}5$ (*left*), $\gamma = 4$ (*middle*) and $\gamma = 16$ (*right*) for time steps (from top to bottom) $t = 50;150;300$. Legend: blue $c = -1$, red $c = 1$

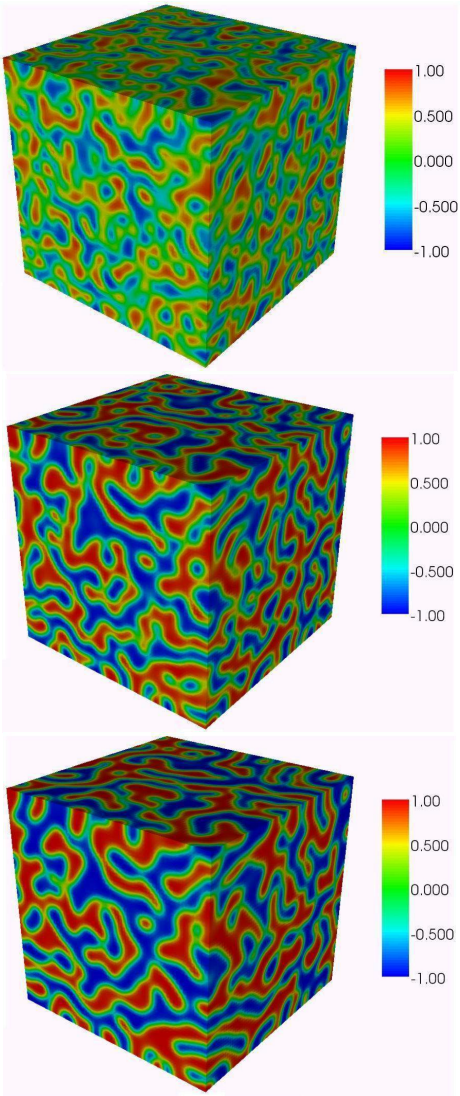

Figure 7 – Solution of the Cahn-Hilliard equation (1,2) in 3D for time steps $t = 40;100;170$

3.2 Cahn-Hilliard equation with logarithmic free energy. For numerical solution $\Omega = [-0,5; 0,5]^2$; $\Delta t = 1 \cdot 10^{-5}$; $t_{final} = 10^{-2}$; $g_1 = -1,3634$; $g_2 = -1,5263$; $g_3 = 0,3630$; $g_4 = 0,1643$; $g_5 = 0,8750$; $\gamma = 10^{-4}$ and $D = 1$. Mesh consists of 64^2 finite elements and initial distribution is random in the interval [0,1; 0,9]. Solution is presented on Fig. 8.

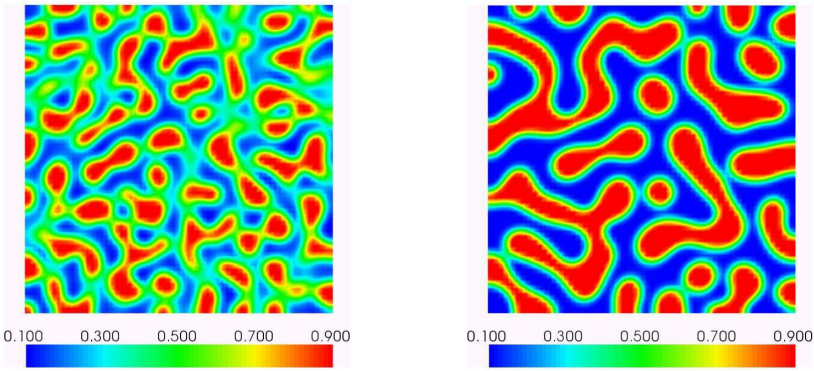

Figure 8 – Solution of Cahn-Hilliard equation with logarithmic free energy (9) for time steps $t = 0.002, 0.01$

4. Outlook. On the numerical side, the primary issue is to account for the strong localization of the phase and concentration boundaries. To assure an efficient discretization of the biharmonic operator, application of Discontinuous Galerkin methods [18, 19, 20] on unstructured meshes is aimed at. Beyond this, it seems that a meshless methods [21, 22, 23] for the spatial discretization of the Cahn-Hilliard equation are perfectly suited for an accurate and highly efficient simulation of these spatially quite heterogeneous problems.

References: **1.** *Danilov D., Nestler B.* Phase-field simulations of solidification in binary and ternary systems using a finite element method // Journal of Crystal Growth. – 2005. – Vol. 275. **2.** *Barrett J. W., Blowey J. F.* Finite element approximation of the Cahn-Hilliard equation with concentration dependent mobility // Math. Comput. – 1999. – Vol. 68. **3.** *Barrett J. W., Blowey J. F.* Finite element approximation of an Allen-Cahn/Cahn-Hilliard system // IMA J. Numer. Anal. – 2002. – Vol. 22. **4.** *French D. A.* Computations on the Cahn-Hilliard model of solidification // Applied Mathematics and Computation. – 1990. – Vol. 40. **5.** *Yeon D.-H., Cha P.-R. et al.* A phase field model for phase transformation in an elastically stressed binary alloy // Modelling and Simulation in Materials Science and Engineering. – 2005. – Vol. 13. **6.** *Uehara T., Fukui M., Ohno N.* Phase field simulations of stress distributions in solidification structures // Journal of Crystal Growth. – 2008. – Vol. 310. **7.** *Ubachs R. L. J. M., Schreurs P. J. G., Geers, M. G. D.* A nonlocal diffuse interface model for microstructure evolution of tin-lead solder // Journal of the Mechanics and Physics of Solids. – 2004. – Vol. 52. **8.** *Ubachs R. L. J. M., Schreurs P. J. G., Geers, M. G. D.* Phase field dependent viscoplastic behaviour of solder alloys // International Journal of Solids and Structures. – 2005. – Vol. 42. **9.** *Ubachs R. L. J. M., Schreurs P. J. G., Geers, M. G. D.* Microstructure dependent viscoplastic damage modelling of tin-lead solder // Journal of the Mechanics and Physics of Solids. – 2006. – Vol. 54. **10.** *Ubachs R. L. J. M., Schreurs P. J. G., Geers, M. G. D.* Elasto-viscoplastic nonlocal damage modelling of thermal fatigue in anisotropic lead-free solder // Mechanics of Materials. – 2007. – Vol. 39. **11.** *Gladkov S., Stiemer M., Svendsen B.* Phase-field-based modeling and simulation of solidification behavior of technological alloys // PAMM. – 2008. – Vol. 8. **12.** *Boettinger W. J., Warren J. A. et al.* Phase-field simulation of solidification // Annual Review of Materials Research. – 2002. – Vol. 32. **13.** *Chen L.-Q.* Phase-field models for microstructure evolution // Annual Review of Materials Research. – 2002. – Vol. 32. **14.** *Granasy L., Pusztai T., Warren J. A.* Modelling polycrystalline solidification using phase field theory // Journal of Physics: Condensed Matter. – 2004. – Vol. 16. **15.** *Cahn J. W., Hilliard J. E.* Free Energy of

a Nonuniform System. I. Interfacial Free Energy // The Journal of Chemical Physics. – 1958. – Vol. 28. **16.** *Elliott C. M., Songmu Z.* On the Cahn-Hilliard equation // Archive for Rational Mechanics and Analysis. – 1986. – Vol. 96. **17.** *Bangerth W., Hartmann R., Kanschat G.* deal.II - A general-purpose object-oriented finite element library // ACM Trans. Math. Softw. – 2007. – Vol. 33. **18.** *Wells G. N., Kuhl E., Garikipati K.* A discontinuous Galerkin method for the Cahn-Hilliard equation // Journal of Computational Physics. – 2006. – Vol. 218. **19.** *Xia Y., Xu Y., Shu C.-W.* Local discontinuous Galerkin methods for the Cahn-Hilliard type equations // Journal of Computational Physics. – 2007. – Vol. 227. **20.** *Stiemer M.* Adaptive finite element simulation of relaxed models for liquid-solid phase transition // Proc. ENUMATH Conference (Graz 2007). **21.** *Рвачев В.Л.* Теория R-функций и некоторые ее приложения. – Киев: Наукова думка, 1982. **22.** *Rvachev V. L., Sheiko T. I.* R-functions in boundary value problems in mechanics // Applied Mechanics Reviews. – 1995. – Vol. 48. **23.** *Belytschko T., Lu Y.Y., Gu L.* Element-free Galerkin methods // International Journal for Numerical Methods in Engineering. – 1994. – Vol. 37

Поступила в редколлегию 30.08.2009

УДК 621.6

А.Ю.ДЕНЬЩИКОВ, асс., ДГМА, Краматорск;
С.В.ПОДЛЕСНЫЙ, канд.техн.наук, доц., ДГМА, Краматорск

СНИЖЕНИЕ КОРОБЛЕНИЙ ПОСЛЕ СВАРКИ МЕТОДОМ ВИБРАЦИОННОГО СТАРЕНИЯ

У статті розглянуто зниження викривлень після зварювання методом вібраційного старіння. Проведені експериментальні дослідження зі зниження зварювальних деформацій для конструкцій що знаходиться у вільному стані та для випадку використання додаткових направляючих. Зроблені висновки про застосовність даного методу для вібраційної правки конструкцій та їх елементів.

In the article the declines of warping are considered after welding of method of vibratory stress relief. Experimental researches are conducted on the decline of welding deformations for the constructions of being in the free state and for the case of the use of the additional sending. Conclusions are done about applicability of this method for the vibratory correction of constructions and their elements.

В последние десятилетия получил распространение способ стабилизации геометрических размеров металлоконструкций под названием «вибрационная обработка» («вибрационное старение»), имеющий ряд преимуществ перед традиционными методами снятия остаточных напряжений [1].

Сущность способа заключается в создании в металлоконструкции после окончательной сборки или в процессе изготовления переменных напряжений определенной величины с помощью специальных вибровозбудителей (вибраторов). Переменные напряжения суммируются с остаточными, и при этом происходит пластическая деформация, способствующая снижению и пере-